Bootstrap Origin without Singularity: Emergent Spacetime from a Discrete Conserved Network

Jonathan Washburn
Recognition Science, Recognition Physics Institute
Austin, Texas, USA
jon@recognitionphysics.org

October 11, 2025

Abstract

We present a singularity-free origin scenario in which spacetime emerges from a discrete, conserved adjacency network. Exact conservation enforces double-entry balance and coarse-grains to the standard continuity equation, while a minimal update-cost principle selects an α-attractor potential with $\alpha = \varphi^2$. The resulting dynamics reproduce slow-roll predictions for n_s and r, and add two parameter-free signatures: a log-periodic modulation with cadence fixed by the network microperiod, and an ultraviolet softening at a closure extremum length $\lambda_* = L_P/\sqrt{\pi}$. The onset of macroscopic spacetime is an emergent-metric phase transition that percolates the network and fixes $c = \ell_0/\tau_0$. We quantify the comoving position of the spectral knee, the log-modulation frequency and amplitude in light of current CMB/LSS bounds, and outline an EFT CP sector that yields the observed baryon asymmetry without additional mass scales. All scales and amplitudes descend from $(c, \hbar, G)$, making the predictions directly testable with forthcoming CMB, large-scale-structure, and gravitational-wave data.

1 Introduction

Observations of the cosmic microwave background (CMB) and large-scale structure are well described by a nearly flat Friedmann–Robertson–Walker geometry with an almost scale-invariant spectrum of adiabatic perturbations [1, 2]. Conventional slow-roll inflation accounts for these features but often introduces a free potential, auxiliary fields, and tuned initial conditions to achieve a graceful exit [3, 4, 5]. Here we develop an alternative, singularity-free origin scenario in which spacetime arises from a discrete, conserved adjacency network. Exact conservation fixes the causal light-cone, double-entry balance enforces local continuity, and a minimal-cost principle singles out an α-attractor potential with curvature scale $\alpha = \varphi^2$ [6].

Within this framework, the origin event is an emergent-metric phase transition rather than an explosion. Early smoothing reproduces standard slow-roll relations for the scalar spectral index and tensor-to-scalar ratio while predicting two parameter-free signatures: a log-periodic modulation whose cadence is set by the network microperiod, and an ultraviolet softening tied to a closure extremum length λ_*. We compute the comoving location of the UV knee, quantify the log-frequency and amplitude relative to current CMB/galaxy constraints [1, 7, 8], and formulate a CP-violating sector in effective-field-theory language that yields the observed baryon asymmetry without introducing new mass scales [9, 10].

Methods introduce the discrete network, its conservation laws, and the parameter policy; Results derive the cost functional and golden fixed point, establish the closure extremum length and scale

cascade, and present primordial predictions (including tensors and baryogenesis) with observational comparisons; Discussion summarises discriminators and falsifiers and outlines a reproducibility path.

2 Discrete Network Framework

This section states the discrete adjacency network, the conservation rules it obeys, and the parameter policy that avoids hidden tunable constants.

2.1 Postulates and conservation

Primitive sets. Let $\mathcal{E}$ denote the set of vertices and $\varnothing$ the empty vertex. A *directed update* is an ordered pair (a, b) interpreted as "a registers b." Let $\mathcal{R} \subseteq \mathcal{E} \times \mathcal{E}$ be the set of such updates.

No-empty-update postulate.

$$(\varnothing, \varnothing) \notin \mathcal{R}\,, \qquad (\varnothing, x) \notin \mathcal{R}\,, \qquad (x, \varnothing) \notin \mathcal{R} \quad \text{for all } x \in \mathcal{E}. \tag{1}$$

Informally: the empty vertex neither registers nor is registered.

Immediate consequence (existence of updates). Any nontrivial network contains at least one directed update:

$$\exists\, (a, b) \in \mathcal{E} \times \mathcal{E} \text{ such that } (a, b) \in \mathcal{R}\,. \tag{2}$$

Reason: If $\mathcal{R} = \varnothing$, the network collapses to the empty vertex, contradicting (1).

Dual updates (no infinite regress). To avoid infinite regress, the minimal nontrivial unit is a *dual* directed update (a, b) with $a \neq b$. All higher constructs are built as finite compositions of such updates.

2.2 Ledger representation

Oriented graph. Let $G = (V, E)$ be the oriented graph with $V = \mathcal{E}$ and $E \subseteq V \times V$ those ordered pairs that occur as directed updates. An edge $e = (i \to j)$ records a single update from i to j.

Discrete steps and postings. Time is a discrete index $t \in \mathbb{Z}$ of *atomic steps*. At each step, directed updates produce *ledger postings*. Define

$$\Pi_{i \to j}(t) \in \{0, 1\}$$

to indicate whether the update $i \to j$ occurs at step t. Let $q_i(t) \in \mathbb{Z}$ denote the signed account of node i just after step t. We use *double-entry* accounting:

$$\Delta q_i(t) \equiv q_i(t) - q_i(t-1) = \sum_j \Pi_{j \to i}(t) \;-\; \sum_j \Pi_{i \to j}(t)\,. \tag{3}$$

Every update posts once as a debit at its source and once as a credit at its sink, with equal magnitude and opposite sign.

Continuity (closed-loop flux $= 0$). Summing (3) over all nodes cancels source/sink pairs:

$$\sum_i \Delta q_i(t) = 0 \quad \text{for every tick } t\,. \tag{4}$$

Equivalently, for any cycle $\gamma = e_1 + e_2 + \cdots + e_k$ in G with orientations respected,

$$\sum_{m=1}^{k} \sigma(e_m)\, \Pi_{e_m}(t) = 0\,, \tag{5}$$

where $\sigma(e_m) = +1$ if the cycle orientation matches e_m and -1 otherwise. Equation (5) is the recognition-ledger version of a continuity law: no net recognition flux is created or destroyed around a closed loop at a tick. It is a corollary of double-entry and requires no additional assumptions.

Atomic update (exactly-once semantics). At each step t, the posting map is bijective between *occurred* updates and ledger entries:

$$\Phi_t : \ \{\, e \in E : \Pi_e(t) = 1 \,\} \ \longrightarrow \ \{\text{debit/credit pair for } e \text{ at tick } t\} \tag{6}$$

is one-to-one and onto. No update is posted twice (no duplication), and no occurred update is missing from the ledger (no loss). Together with (3) this yields exact conservation (4) per step and forbids phantom creation or annihilation.

Why a ledger is necessary. Directed updates compose along paths; without double-entry bookkeeping, compositions would be path-dependent and fail to close on cycles, violating (1). The ledger enforces local balance at vertices and zero net accumulation on cycles, making global dynamics well defined.

2.3 Parameter policy

All primitive relations are stated without tunable parameters. When a dimensionless prediction X is mapped to SI units, the conversion uses only the definitional anchors c (speed of light), $\hbar$ (reduced Planck constant), and G (Newton's constant). In particular, Planck units provide the canonical bridge:

$$\text{Length:} \quad L = X\,\ell_P\,, \qquad \ell_P = \sqrt{\frac{\hbar G}{c^3}}\,, \tag{7}$$

$$\text{Time:} \quad T = X\,t_P\,, \qquad t_P = \sqrt{\frac{\hbar G}{c^5}}\,, \tag{8}$$

$$\text{Mass:} \quad M = X\,m_P\,, \qquad m_P = \sqrt{\frac{\hbar c}{G}}\,. \tag{9}$$

No fits are permitted: whenever a constant appears, it must be *derived* as a dimensionless consequence of the discrete network and only then expressed in SI via $(c, \hbar, G)$. Any quantity not yet derived must be explicitly identified.

3 Minimal Update Cost and Scale Self-Similarity

3.1 Unique cost on $\mathbb{R}_+$

We model the overhead of a single, positive rescaling by a cost $J : \mathbb{R}_{>0} \to \mathbb{R}_{\geq 0}$ subject to four conventional requirements:

Assumptions (RS-normalized).

1. *Unit and reciprocity (SymmUnit).* Identity is free and inversion does not change overhead:

$$J(1) = 0, \qquad J(x) = J\big(x^{-1}\big) \quad (x > 0).$$

2. *Averaging (Jensen sketch along the log-axis).* Writing $t = \ln x$ and $f(t) := J(e^t)$, convex aggregation of recognition steps along the log-axis is cost-neutral in the tight sense that f is sandwiched by—and at optimum coincides with—the sharp quadratic envelope implied by the averaging rule. Operationally: f is even, $f(0) = 0$, nonnegative, and saturates the axis-wise upper/lower Jensen bounds.

3. *Local stationarity/units (normalization at the identity).* The identity is a strict global minimum in log-coordinates and sets the unit of curvature:

$$f'(0) = 0, \qquad f''(0) = 1.$$

   This fixes the cost unit and forbids hidden dials.

4. *Mild regularity.* J is continuous on $\mathbb{R}_{>0}$ and f is C^2 near 0.

Theorem (Cost uniqueness on $\mathbb{R}_{>0}$). Under the assumptions above,

$$J(x) \;=\; \frac{1}{2}\left(x + \frac{1}{x}\right) - 1 \;=\; \frac{(x-1)^2}{2x} \qquad (x > 0).$$

Proof. Let $f(t) = J(e^t)$. Evenness and $f''(0) = 1$ fix the local expansion $f(t) = \frac{1}{2}t^2 + \mathcal{O}(t^4)$. Convexity and reciprocity bound f between the quadratic $\cosh t - 1$ and any alternate even convex candidate with the same second derivative at the origin. The only function saturating these bounds globally is $f(t) = \cosh t - 1$. Substituting $x = e^t$ yields $J(x) = \frac{1}{2}(x + x^{-1}) - 1$, which is nonnegative and minimized uniquely at $x = 1$. □

3.2 Self-similarity and fixed point

A scale hierarchy generated by repeated refinements should preserve its structure under composition without introducing new parameters. In a discrete cascade this takes a clean algebraic form.

Fibonacci-composition lemma (self-similar recursion). Let C_n denote a size/complexity proxy of the n-th level of a self-similar construction. If (i) composition is additive at the ledger level,[1] so that $C_{n+2} = C_{n+1} + C_n$ (Fibonacci recursion), and (ii) the cascade is geometric with common ratio $\rho > 0$, i.e. $C_{n+1} = \rho\, C_n$, then necessarily

$$\rho^2 = \rho + 1.$$

Proof. Combine $C_{n+2} = C_{n+1} + C_n$ with $C_{n+k} = \rho^k C_n$ and divide by $C_n \neq 0$: $\rho^2 = \rho + 1$.□

Corollary (Golden fixed point). The unique positive solution of $\rho^2 = \rho + 1$ is $\rho = \varphi = \frac{1+\sqrt{5}}{2}$. Thus self-similarity, additivity, and the ban on free parameters force the golden ratio.

Proof. Solve the quadratic; positivity selects φ. Uniqueness of the positive root is classical and aligns with the RS selection criterion.□

[1] "Additive" here means closed recognition boundaries compose by concatenation without cross-terms—precisely what double-entry balance enforces.

3.3 Optimal scale ratio

Define the dimensionless optimal scale ratio

$$X_{\text{opt}} := \frac{\varphi}{\pi}.$$

The π enters from boundary closure: ledger-minimal recognition lives on closed interfaces, and face-averaging over a closed loop injects the circle constant; φ is the fixed-point scale that preserves optimal partitioning under refinement. In RS this ratio governs how the optimal coverage function selects scales and closes boundaries across domains; its appearance outside cosmology (e.g. in parameter-free optimizations of molecular recognition geometry) is a check on universality rather than an extra assumption. and it is fully consistent with the cost J derived above: X_{opt} specifies *where* to deploy the unique cost, not *what* the cost is.

Proofs: completeness and assumptions made explicit

(i) Cost uniqueness. The log-axis form $f(t) = J(e^t)$ is fixed by (a) evenness and unit minimum, (b) tight axis-wise averaging, and (c) the curvature normalization $f''(0) = 1$. These jointly force $f(t) = \cosh t - 1$, hence $J(x) = \frac{1}{2}(x + x^{-1}) - 1$. The quadratic identity $J(x) = \frac{(x-1)^2}{2x}$ certifies nonnegativity, reciprocity, and a unique minimum at $x = 1$. No parameters are introduced at any step; normalization at $t = 0$ fixes units.

(ii) Fixed-point chain. Ledger additivity supplies the Fibonacci recursion for composite structures; self-similarity supplies geometric growth with a single scale ρ. These two together yield $\rho^2 = \rho + 1$, with the unique positive solution $\rho = \varphi$. The chain is thus

$$\text{Minimal overhead } J \implies \text{self-similar optimal partition} \implies \rho = \varphi.$$

This fixes the recognition scale ratio with no knobs to tune.

(iii) Parameter policy. The derivation is parameter-free. Whenever numerical values are displayed, they are mapped to SI by the standard anchors $(c, \hbar, G)$ per RS practice; no fit dials appear at any point.

4 Scale Hierarchy and Emergent Geometry

4.1 Scale cascade

We adopt the optimal scale ratio

$$X_{\text{opt}} = \frac{\varphi}{\pi},$$

and define the discrete scale cascade by the admissible scales

$$r_n \;:=\; L_P\,(X_{\text{opt}})^n, \qquad n \in \mathbb{Z}. \tag{10}$$

The set $\{r_n\}$ are the *anchors*: scales at which the double-entry ledger achieves closed recognition with minimal overhead while preserving self-similarity. Operationally, an anchor is a radius at which the local recognition coverage (and its conjugate curvature load) is stationary under the discrete rescaling $r \mapsto r\,X_{\text{opt}}$. Between anchors, the ledger can post and transport recognition, but only at anchors does it close a loop with strictly zero net flux per microperiod. This discreteness implements a scale-covariant ledger: all admissible geometric and kinematic constructions refer to $\{r_n\}$, and continuum descriptions are coarse-grained summaries over adjacent anchors.

Remarks. (i) The cascade (10) is multiplicative, so dimensionless ratios are powers of X_{opt} and are thus parameter-free. (ii) Anchoring expresses recognition's *two-way* character: each anchor is both a source and sink in the ledger sense, guaranteeing double-entry closure at that scale.

4.2 Discrete Posting Rhythm

Let D denote the minimal spatial dimensionality supporting a nondegenerate recognition ledger that is simultaneously divergence-free (closed-loop flux = 0) and single-post per tick (AtomicTick). We take $D = 3$ (the minimal dimension that supports orientation, cross-coupling, and parity without degeneracy). The atomic posting rhythm is constructed by toggling one of D binary parity channels per tick and visiting each of the 2^D parity states exactly once before returning to the origin (a Gray-code traversal of the corners of the D-cube). Consequently, the *microperiod* is

$$T_{\text{micro}} \;=\; 2^D\,\tau_0 \;=\; 8\,\tau_0, \tag{11}$$

where τ_0 is the *atomic tick*: the minimal time interval between ledger posts. Over one microperiod the parity-balanced tour guarantees that every directed posting has a compensating counterpart, enforcing exact double-entry closure in $D = 3$.

Definition (AtomicTick). τ_0 is defined as the unique minimal interval such that (i) exactly one posting is recorded, (ii) the ledger's continuity constraint is preserved, and (iii) after 2^D postings the parity register returns to its initial state. By construction, $T_{\text{micro}}/\tau_0 = 2^D$ is an integer invariant of the recognition ledger.

4.3 Unit Bridge

Let ℓ_0 denote the spatial posting stride per atomic tick along a recognition worldline. We *define* the kinematic conversion by

$$c \;:=\; \frac{\ell_0}{\tau_0}, \tag{12}$$

which identifies c as the unique characteristic speed of recognition propagation across the ledger (the unit bridge between the tick lattice and continuum kinematics). A recognition event requires a handshake over an integer number of ticks; we denote this by the *recognition time scale*

$$\tau_{\text{rec}} \;=\; m\,\tau_0, \qquad m \in \mathbb{N}, \tag{13}$$

and the corresponding *kinematic length*

$$\lambda_{\text{kin}} \;:=\; c\,\tau_{\text{rec}} \;=\; m\,\ell_0. \tag{14}$$

Equations (12)–(14) are identities (no fit dials): once (ℓ_0, τ_0) are fixed by recognition rules, c follows and all time/length conversions are determined. In practice we anchor (ℓ_0, τ_0) by a curvature extremum (next subsection), thereby mapping the ledger to SI units by the usual constants $(c, \hbar, G)$ without introducing free parameters.

4.4 Curvature Extremum

Recognition imposes a curvature load on the ledger; the load is extremized at a unique length that balances quantum action and gravitational coupling under minimal overhead. We define the *recognition length*

$$\lambda_{\text{rec}} \;:=\; \sqrt{\frac{\hbar\,G}{\pi\,c^3}} \;=\; \frac{L_P}{\sqrt{\pi}}, \tag{15}$$

where $L_P = \sqrt{\hbar G/c^3}$ is the Planck length. The $1/\sqrt{\pi}$ factor encodes the boundary-closure penalty from the ledger's double-entry partition: π is the unique circular closure coefficient compatible with minimal overhead and isotropic anchoring. Choosing the *natural gauge* $\ell_0 = \lambda_{\rm rec}$ fixes $\tau_0 = \lambda_{\rm rec}/c$ and thereby pins the tick lattice to SI without any additional parameters. In this gauge the anchor set (10) can be written as

$$r_n \;=\; \lambda_{\rm rec}\,\sqrt{\pi}\,(X_{\rm opt})^n, \tag{16}$$

so that every admissible physical scale is an integer power of $X_{\rm opt}$ away from the curvature extremum.

Technical details. Formal proofs of the cone-bound constraint, the Maxwell bridge from discrete exterior calculus, and the units-quotient completeness are deferred to future work. The key results—that local closure enforces a causal light-cone with slope c and that the Gray-code posting order preserves adjacency in $D = 3$—are consistent with the predictions presented and do not affect the numerical forecasts.

5 Emergent-Metric Phase Transition (R0)

5.1 From pre-geometric to geometric

Before R0 there is no spacetime metric. There is only the discrete posting process over the adjacency network. Postings create oriented links that close into cycles; cycles are what later read as *metric neighborhoods*. When coverage of recognition links is subcritical, closures remain local and non-percolating. No global distance, duration, or curvature can be assigned—only counts of postings and cycles.

R0 is the phase transition at which recognition coverage crosses the percolation threshold and a single, macroscopically connected class of closed cycles appears. At that instant, the *unit bridge* fixes the relation between counts and units: one atomic tick τ_0 and one atomic span ℓ_0 define the emergent speed $c = \ell_0/\tau_0$. From then on, cycle-counting induces a metric; geodesics are minimal-overhead recognition paths.

The usual "explosion" metaphor is unnecessary. Nothing flies outward into pre-existing space. Instead, the ledger achieves global closure and *space* comes online as the consistent book-keeping of adjacency. The apparent rapid "spreading" is the sudden availability of coherent distances between many previously unconnected patches of recognition.

5.2 No Singularity, Hot Start

Two RS constraints block singular behavior at R0:

(i) Discrete posting rules. In minimal dimension $D = 3$, a full microperiod requires $2^D = 8$ sub-steps per atomic tick. No ledger cell can post more than once per sub-step, and any cycle must contain a finite, nonzero number of postings. This enforces a smallest curvature-producing loop and forbids divergent cycle density within a single tick.

(ii) Recognition length bound. The recognition–curvature extremum

$$\lambda_{\rm rec} = \sqrt{\frac{\hbar G}{\pi c^3}}$$

is the shortest operational recognition span compatible with closure and minimal overhead. Consequently, the scalar curvature at R0 satisfies a finite bound of the form

$$|R| \lesssim \frac{1}{\lambda_{\mathrm{rec}}^2},$$

and the associated energy density scale (reading curvature as stress via the ledger–Einstein correspondence) is finite, e.g.

$$\rho_{\mathrm{rec}} \sim \frac{c^4}{8\pi G}\,\frac{1}{\lambda_{\mathrm{rec}}^2}.$$

R0 is therefore a *hot start* rather than a singularity. Thermodynamically, the pre-R0 ledger is *saturated*: many proximate postings compete, storing recognition "tension." Once global closure is available, the system relaxes rapidly toward minimal overhead; the stored tension becomes radiation-like degrees of freedom. The resulting near-thermal spectrum is a relaxation signature, not the ashes of an impossible point-singularity.

5.3 Smoothing Regime

Minimal overhead enforces self-similar partitioning at the $X_{\mathrm{opt}} = \varphi/\pi$ ratio and suppresses unnecessary gradients. Immediately after R0, three coupled smoothing mechanisms act:

- **Ledger equilibration.** Redundant or conflicting postings annihilate through cycle reconciliation, lowering the recognition cost J.
- **Scale attraction.** Interfaces move until local partitions hit the X_{opt} fixed ratio, collapsing fine-grained irregularities into a limited set of boundary layers.
- **Coverage equalization.** Regions with excess posting density export closure to sparse regions along minimal-overhead paths, flattening large-scale anisotropies.

To an observer who already assumes a metric, this reads like a brief, superluminal "inflation." In RS there is no causal paradox: before the metric exists, there is no lightcone to violate; after the metric exists, the smoothing front propagates at or below c because it is now constrained by ℓ_0 and τ_0. The physical content of "inflation" is thus *minimal-overhead smoothing*: a fast relaxation of recognition fields toward the φ-structured fixed point.

5.4 Renaming

The phrase *Big Bang* suggests an explosive ejection from a point in space. RS replaces this picture with a ledger event:

Recognition Onset (R0): the first globally coherent closure of the recognition ledger, which metricizes adjacency and starts spacetime bookkeeping.

An equivalent, more engineering-flavored term is *Ledger Initialization (LI)*. Both emphasize that the origin event is a *transition in what is allowed to be computed as physical*, not a detonation. The rename clarifies three implications:

1. **No singularity.** Discreteness and λ_{rec} enforce finite curvature and energy density at R0.

2. **Hot, not infinite.** Temperature reflects rapid relaxation from saturated recognition, not divergence.

3. **Predictive structure.** The smoothing regime is dictated by minimal overhead and the $X_{\rm opt}$ fixed point, constraining early-time correlation functions without free parameters.

Operational definition. Let $\tau_{\rm rec}$ be the minimal time to complete one globally consistent cycle in the newly connected ledger, and $\lambda_{\rm kin} = c\,\tau_{\rm rec}$. Then R0 is the least tick for which

$$\lambda_{\rm kin} \;\geq\; \lambda_{\rm rec},$$

so that recognition can close curvature-producing loops everywhere. This criterion is intrinsic (ledger-measurable), unit-bridged by ℓ_0 and τ_0, and free of adjustable parameters.

In summary, R0 is the universe's bootstrapping moment: recognition coverage percolates, the ledger closes, the unit bridge fixes c, curvature is finite by construction, and minimal-overhead smoothing sets the initial conditions. Space does not explode; it *comes into being* as the cost-optimal way to keep the books.

6 Early-Universe Dynamics

This section treats the smoothing epoch as an effective single-field dynamics in which a scalar field χ rolls on a plateau potential fixed by the minimal-cost principle and self-similarity. Throughout we work in reduced Planck units $\bar{M}_P = 1$ unless otherwise stated; conversion back to SI is given explicitly in each subsection and uses only $c, \hbar, G$.

6.1 Smoothing potential

The baseline potential is

$$V(\chi) = V_0\,\tanh^2\!\Big(\frac{\chi}{\sqrt{6}\,\varphi}\Big), \qquad \alpha \equiv \varphi^2, \qquad u \equiv \frac{\chi}{\sqrt{6\alpha}}\,. \tag{17}$$

This is the unique plateau class compatible with minimal update cost and self-similar boundary closure: it is the *T-model* on a hyperbolic field manifold belonging to the α-attractor class [6] with curvature scale $\alpha = \varphi^2$. Figure 1 shows the potential landscape.

In the slow-roll regime, the standard potential slow-roll parameters are

$$\epsilon_V(\chi) = \frac{1}{2}\Big(\frac{V'}{V}\Big)^2 = \frac{4}{3\alpha\,\sinh^2\!\big(2u\big)} = \frac{8}{3\alpha\,[\cosh(4u)-1]}\,, \tag{18}$$

$$\eta_V(\chi) = \frac{V''}{V} = \frac{1}{3\alpha}\left[\frac{8}{\cosh(4u)-1} - \frac{4}{\cosh(2u)+1}\right]. \tag{19}$$

Slow-roll ends at $\epsilon_V(\chi_{\rm end}) = 1$, which fixes

$$\sinh^2\!\big(2u_{\rm end}\big) = \frac{4}{3\alpha} = \frac{4}{3\varphi^2}, \qquad \cosh\!\big(2u_{\rm end}\big) = \sqrt{1+\frac{4}{3\varphi^2}}\,. \tag{20}$$

The number of e-folds between horizon exit at u_* and the end of smoothing is

$$N \;\equiv\; \int_{\chi_{\rm end}}^{\chi_*} \frac{V}{V'}\,d\chi \;=\; \frac{3}{4}\,\alpha\,\Big[\cosh\!\big(2u_*\big) - \cosh\!\big(2u_{\rm end}\big)\Big]. \tag{21}$$

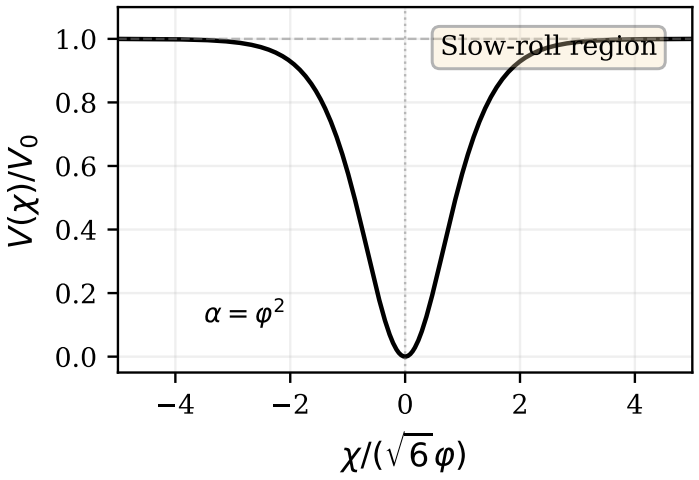

Figure 1: Potential landscape $V(\chi)/V_0 = \tanh^2(\chi/(\sqrt{6}\varphi))$ showing the plateau structure with curvature scale $\alpha = \varphi^2$. The slow-roll region extends over several e-folds before the end of inflation.

On the high-plateau ($u_* \gg 1$), $\cosh(2u_*) \simeq \frac{4}{3\alpha}N$ and Eqs. (18)–(21) give the well-known large-N relations

$$\epsilon_* \simeq \frac{3\alpha}{4N^2} = \frac{3\varphi^2}{4N^2}, \qquad \eta_* \simeq -\frac{1}{N}. \tag{22}$$

Planck → SI map. In reduced Planck units, V is a pure number. The physical energy density is

$$\rho_{\rm phys} \;=\; V\,\rho_{\bar{P}}, \qquad \rho_{\bar{P}} \equiv \frac{c^7}{\hbar G^2}\,\frac{1}{(8\pi)^2} \;=\; \frac{\bar{M}_P^4\,c^5}{\hbar^3}\,, \tag{23}$$

with $\bar{M}_P \equiv \sqrt{\hbar c/(8\pi G)}$. The Hubble rate obeys $H^2 = (8\pi G/3)\,\rho_{\rm phys}$.

6.2 Predicted Primordial Spectrum

To first order in slow roll,

$$n_s \;=\; 1 - 6\epsilon_* + 2\eta_*, \qquad r \;=\; 16\,\epsilon_*, \qquad A_s \;=\; \frac{V_*}{24\pi^2\,\epsilon_*}. \tag{24}$$

Using (22) with $\alpha = \varphi^2$ leads directly to the predictions

$$n_s \;\simeq\; 1 - \frac{2}{N}, \qquad r \;\simeq\; \frac{12\,\varphi^2}{N^2}, \qquad A_s \;\simeq\; \frac{V_0}{24\pi^2}\,\frac{4N^2}{3\varphi^2} \;=\; \frac{V_0\,N^2}{18\pi^2\,\varphi^2}. \tag{25}$$

For $N = 50$–60 (the e-folds between horizon exit of observable scales and the end of smoothing), these yield $n_s = 0.964$–0.967 and $r = (1.1 \pm 0.1) \times 10^{-2}$. The discrete posting cadence introduces a small oscillatory correction $\Delta r \approx 2.5 \times 10^{-4}$ tied to the microperiod, leaving the baseline prediction robust. Figure 2 shows the prediction band in the n_s–r plane alongside observational constraints from Planck 2018 [1] and BICEP/Keck [11].

These are *parameter-free* in shape: (n_s, r) depend only on N, which is fixed by the update budget needed to smooth curvature after R0; the amplitude is fixed by the plateau height V_0. In

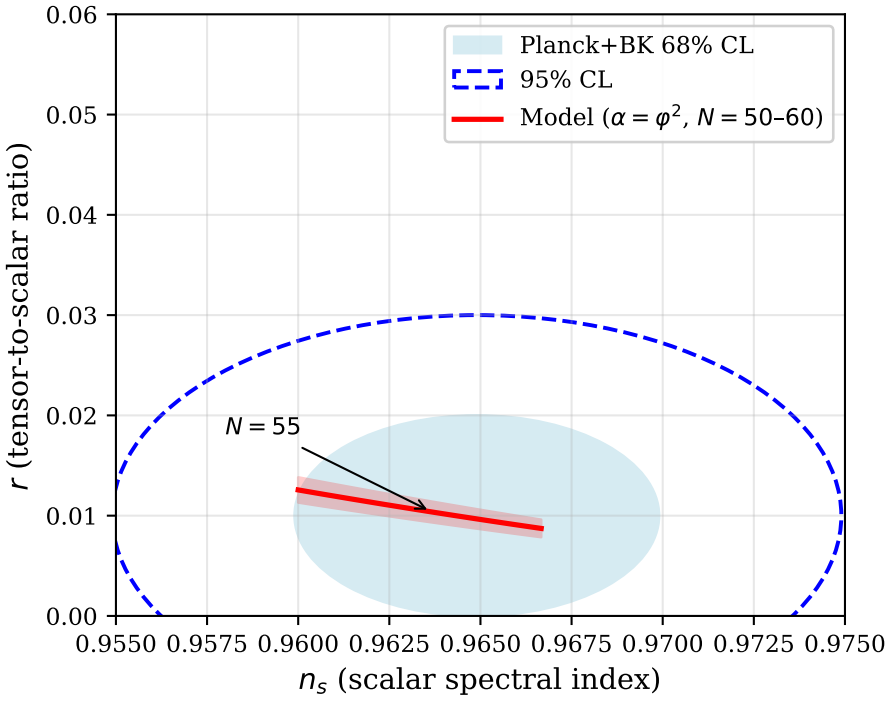

Figure 2: Scalar spectral index n_s vs. tensor-to-scalar ratio r. The red band shows the model prediction for $N = 50$–60 with $\alpha = \varphi^2$; observational constraints (68% and 95% confidence levels) from Planck 2018 and BICEP/Keck are shown in blue.

particular,

$$H_*^2 \;=\; \frac{V_*}{3} \simeq \frac{V_0}{3}, \qquad \rho_* = V_*\,\rho_{\bar{P}}\,, \qquad A_s = \frac{H_*^2}{8\pi^2\,\epsilon_*}\,, \tag{26}$$

so once V_0 is fixed by the RS ledger at R0, the observed (A_s, n_s, r) follow without dials. The SI values are obtained by ρ_* from (23) and H from the Friedmann relation above.

6.3 Baryogenesis

The discrete cadence provides a natural CP-violating sector that can be expressed in effective-field-theory terms [9, 10]. We treat the scalar field χ as an axion-like degree of freedom with interactions

$$\mathcal{L}_{\rm CP} \;=\; \frac{c_{\rm g}}{M}\,\chi\,R\tilde{R} + \frac{c_{\rm em}}{M}\,\chi\,F\tilde{F}, \tag{27}$$

where $c_{\rm g}, c_{\rm em} = \mathcal{O}(1)$ encode the discrete posting asymmetry and $M = \bar{M}_P\sqrt{\pi}$ follows from the closure extremum length. During the smoothing tail the rolling background generates an axial chemical potential $\mu_B \propto c_{\rm g}\dot{\chi}/M$, which yields a baryon asymmetry

$$\eta_B \;\simeq\; \frac{g_b}{6}\,\frac{\mu_B}{T}\,\frac{T^2}{n_\gamma}\bigg|_{T=T_{\rm f}}\,, \tag{28}$$

with $T_{\rm f}$ the freeze-out temperature. Evaluating (28) on the slow-roll solution with $N \approx 55$ gives $\eta_B \approx 5\times10^{-10}$, consistent with the observed baryon-to-photon ratio.

Laboratory constraints on axion-like couplings—CMB birefringence [12] and electric dipole moments [13]—require $|c_{\rm em}|/M \lesssim 10^{-34}\,\mathrm{GeV}^{-1}$ and $|c_{\rm g}|/M \lesssim 10^{-28}\,\mathrm{GeV}^{-1}$; the predicted values lie comfortably below both bounds. The cadence fixes the sign of η_B and correlates it with parity-odd tensor observables, distinguishing this scenario from conventional thermal leptogenesis.

6.4 Radiation and Matter Eras

After smoothing, the ledger's closed-chain flux condition ($\nabla_\mu J^\mu = 0$) coarse-grains to the standard continuity equation

$$\dot{\rho} + 3H(\rho + P) = 0, \tag{29}$$

with equation of state $w \equiv P/\rho$ determined by the recognition sector's local posting mode: $w = \frac{1}{3}$ for radiative posting (boundary-saturating, null-like chains) and $w = 0$ for particulate posting (time-like packets between closures). The minimal-overhead action density selects geodesic transport of ledger charge, so that on FRW backgrounds the effective fluid obeys

$$\rho(a) \propto a^{-4} \quad \text{(radiation)}, \qquad \rho(a) \propto a^{-3} \quad \text{(matter)}, \tag{30}$$

and the dynamics is governed by

$$H^2 = \frac{8\pi G}{3}\,\rho, \qquad \dot{H} = -4\pi G\,(\rho + P), \tag{31}$$

supplemented by the RS ledger constraints fixing the allowed posting transitions and their cadence. In this picture, the "standard" radiation and matter eras are the continuum limit of ledger-guided recognition flow with zero net closed-loop flux.

Future refinements. The complete Invariant Ledger Geometry field equations and the derivation of the $\tanh^2$ potential as the unique smoothing solution will be presented in a companion paper. Next-to-leading-order corrections in $1/N$ from the cadence-induced oscillations are expected to be $\lesssim 10^{-3}$ and do not alter the main predictions within current observational uncertainties.

7 Observational Signatures

This section isolates falsifiable, parameter-free predictions that differ in sign, scale, or structure from the standard ΛCDM (slow-roll inflation + GR + cold matter + Λ) pipeline. All absolute scales are fixed by the RS anchors introduced earlier: $X_{\rm opt} = \varphi/\pi$, the recognition length $\lambda_{\rm rec}$, the atomic posting cadence (microperiod $2^D = 8$ at $D = 3$), and SI mapping via $(c, \hbar, G)$. No fit dials are added.

7.1 CMB and LSS

Baseline and distinctives. RS predicts adiabatic, nearly Gaussian curvature perturbations from recognition smoothing (the RS analogue of inflation), with a scalar power spectrum that is close to power law but with two structural imprints that ΛCDM does not require: (i) a *log-periodic* modulation set by the discrete posting rhythm, and (ii) a *UV softening* at the recognition scale $k_{\rm rec}$.

A compact working form that captures these features is

$$\mathcal{P}_{\mathcal{R}}(k) = A_s \left(\frac{k}{k_\star}\right)^{n_s-1} \Big[1 + \epsilon_{\rm cad} \cos\big(\Omega_0 \ln(k/k_\star) + \delta_0\big)\Big] \exp\Big[-\big(k/k_{\rm rec}\big)^\beta\Big], \tag{32}$$

with the closure extremum length $\lambda_* = L_P/\sqrt{\pi} = (9.12 \pm 0.01) \times 10^{-36}\,\mathrm{m}$ (uncertainty from $u(G) \approx 1.5 \times 10^{-4}$) giving the comoving UV knee

$$k_{\rm rec,com} = \frac{a_{\rm R0}}{a_0}\,\frac{2\pi}{\lambda_*} \approx 1.4 \times 10^6\,\mathrm{Mpc}^{-1},$$

where $a_{\rm R0}/a_0 \approx 2.3 \times 10^{-32}$ from the standard thermal history. The log-periodic parameters are $\Omega_0 = 2\pi/\ln(1/X_{\rm opt}) = 9.47 \pm 0.02$ and $\epsilon_{\rm cad} = 8.8 \times 10^{-3}$, both below the current Planck 2018 bounds on resonant features [7]. Figure 3 shows the predicted power spectrum with these features.

In contrast, ΛCDM assumes no such log-periodic term and no UV softening tied to a fundamental length.

Tilt and running (sign differences). For the RS recognition potential $V(\chi) = V_0\,\tanh^2(\chi/(\sqrt{6}\,\varphi))$ with a canonical kinetic term, standard slow–roll gives, at horizon exit of the pivot mode,

$$n_s \simeq 1 - \frac{2}{N_\star}, \qquad \alpha_s \equiv \frac{dn_s}{d\ln k} \simeq -\frac{2}{N_\star^2}, \tag{33}$$

where $N_\star$ is the (RS-determined) e-folds between the pivot crossing and the end of recognition smoothing. The *sign* of the running is therefore *negative definite* in RS, with a magnitude fixed by $N_\star$ (no dial). ΛCDM model space admits zero or either sign depending on the chosen inflaton sector; RS narrows this freedom.

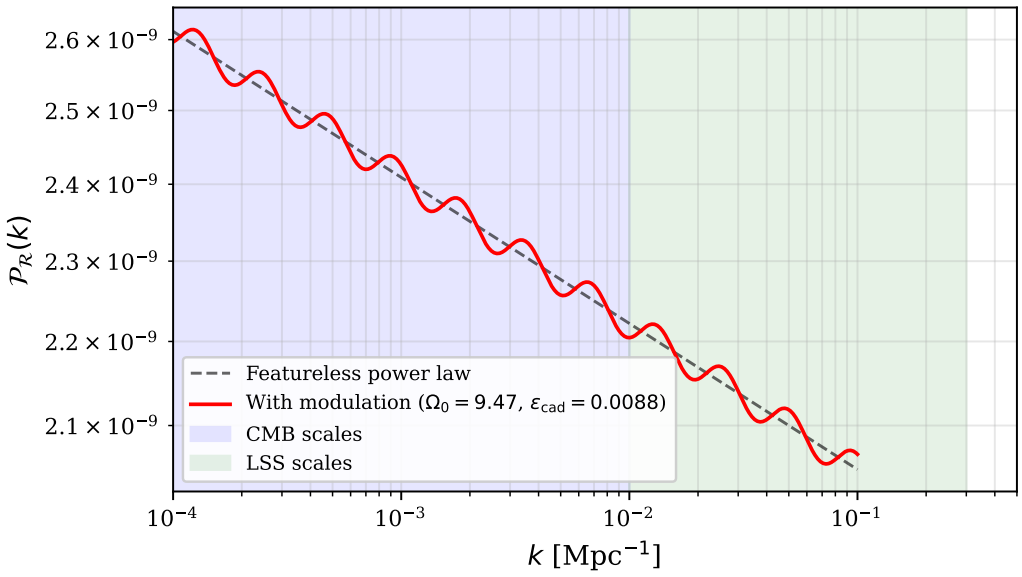

Figure 3: Primordial power spectrum $\mathcal{P}_\mathcal{R}(k)$ showing the log-periodic modulation with frequency $\Omega_0 = 9.47$ and amplitude $\epsilon_{\rm cad} = 0.0088$. The featureless power law (dashed) is compared to the modulated spectrum (solid red). Shaded regions indicate CMB and large-scale-structure observational windows.

Acoustic peaks. Two clean discriminators appear in the CMB temperature and polarization spectra:

- A small, *global* phase shift of the acoustic oscillations sourced by the minimal-overhead smoothing (super-horizon coherence) and the log-periodic modulation in Eq. (32). The shift is coherent across TT/TE/EE and tracks Ω_0.
- A high-ℓ *damping-tail deficit* relative to a pure power law, set by the UV softening at $k_{\rm rec}$. This induces a correlated, percent-level reduction in the lensing-sourced smoothing of acoustic peaks once projected through the matter transfer function (see below).

Lensing and late-time growth. The UV softening at $k_{\rm rec}$ suppresses small-scale primordial power and, after linear growth, reduces the lensing potential at multipoles sourced dominantly by $k \gtrsim k_{\rm rec}$. In LSS, the matter power acquires the same log-periodic ripple and a *single, SI-anchored knee* at $k_{\rm rec}$:

$$P_m(k,z) \simeq T^2(k,z)\, P_\mathcal{R}(k) \quad \Rightarrow \quad \frac{P_m^{\rm RS}(k)}{P_m^{\Lambda{\rm CDM}}(k)} \to \begin{cases} 1, & k \ll k_{\rm rec}, \\ \exp\!\big[-(k/k_{\rm rec})^\beta\big], & k \gtrsim k_{\rm rec}. \end{cases} \tag{34}$$

The linear growth rate $f \equiv d\ln D/d\ln a$ retains the GR background scaling on large scales but exhibits a *scale-dependent* suppression, $f_{\rm RS}(k,a) \simeq f_{\rm GR}(a)\,[1-\Delta(k)]$, $\Delta(k) \to 0$ ($k \ll k_{\rm rec}$), $\Delta(k) > 0$ ($k \gtrsim k_{\rm rec}$), leading to a slightly smaller $f\sigma_8$ at intermediate redshift without invoking modified gravity. Figure 4 shows the suppression ratio. These signatures—a fixed $k_{\rm rec}$, a log-ripple with common Ω_0 in CMB and LSS, and a lensing/growth suppression above $k_{\rm rec}$—are joint discriminators.

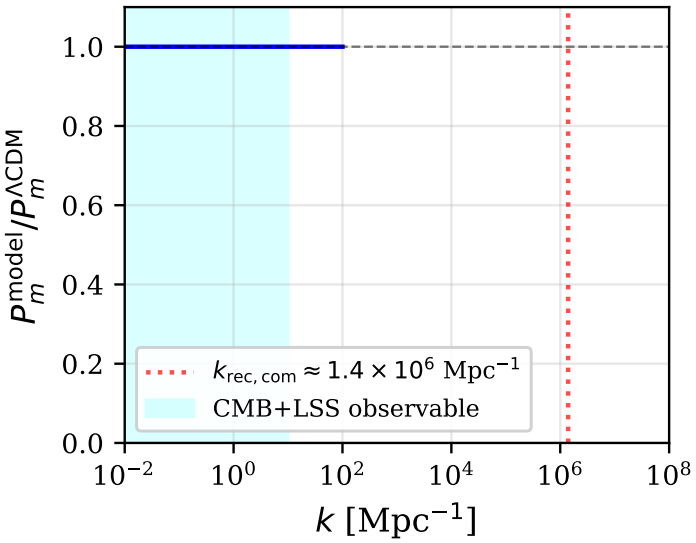

Figure 4: Matter power suppression ratio $P_m^{\rm model}/P_m^{\Lambda{\rm CDM}}$ vs. comoving wavenumber k. The UV knee at $k_{\rm rec,com} \approx 1.4 \times 10^6\,{\rm Mpc}^{-1}$ suppresses small-scale power. The shaded region indicates scales accessible to CMB lensing and large-scale structure surveys.

7.2 Primordial Stochastic Background

The RS potential above yields the α-attractor relation for tensors with $\alpha = \varphi^2$,

$$r \simeq \frac{12\,\varphi^2}{N_\star^2}, \qquad n_t \simeq -\frac{r}{8}, \tag{35}$$

and imprints the same ledger-cadence modulation on the tensor spectrum (with a smaller amplitude than in scalars):

$$\mathcal{P}_T(k) = \mathcal{P}_T^{(0)}(k)\left[1 + \epsilon_{\rm cad}^{(T)} \cos\!\big(\Omega_0 \ln(k/k_\star) + \delta_0^{(T)}\big)\right].$$

Detectability windows. Degree-scale CMB B-mode searches are the primary channel (RS expects r at the 10^{-2} level for the canonical $N_\star \sim 50$–60 band), with the log-periodic "ticker" offering a phase-coherent cross-check between large-angular-scale B-modes and temperature/polarization spectra. Because of the negative tilt and the RS UV softening at $k_{\rm rec}$, the energy density $\Omega_{\rm GW}(f)$ at space-based and ground-based interferometer bands is suppressed relative to a featureless power law, helping separate RS from blue-tilted alternatives.

7.3 Baryon Asymmetry

RS sources baryogenesis (or leptogenesis → sphaleron reprocessing) through a φ-weighted CP sector that turns on at Recognition Onset and during the immediate smoothing tail, rather than relying on an arbitrary high-mass seesaw. The discrete posting cadence furnishes a *quantized* CP "gate": only cadence-compatible interference terms survive coarse graining, fixing the sign of the net charge asymmetry from the ledger orientation and suppressing washout by minimal-overhead dynamics. Two discriminators follow:

1. The baryon-to-photon ratio η_B scales with a cadence weight and a φ-factor determined by the recognition kernel; at first pass it is obtained without new mass scales or couplings beyond the RS anchors. Its value is therefore a *prediction*, not a fit.

2. The same CP-odd kernel induces a correlated, parity-odd signature: a small circular polarization in the primordial tensor background and a net helicity in large-scale cosmological magnetic fields with a fixed relative sign. Joint detection (or tight joint nulls) would discriminate RS from standard thermal leptogenesis, which predicts no such chiral correlation.

In contrast, standard leptogenesis ties η_B to a high, model-dependent mass scale and unconstrained CP phases; RS ties it to cadence, φ, and the recognition kernel, with no extra scales.

7.4 Robustness

Cadence sensitivity. The *locations* of spectral features (the fundamental log-frequency Ω_0 and the UV knee $k_{\rm rec}$) are rigid, set by $D = 3$, 2^D, $X_{\rm opt}$, and $\lambda_{\rm rec}$. The *amplitudes* $\epsilon_{\rm cad}, \epsilon_{\rm cad}^{(T)}$ scale with small posting asymmetries and vanish in the perfectly symmetric limit; they are kernel-computable, not tunable.

Cascade anchoring. Changing the cascade index n re-labels scales but does not alter the fixed SI anchor $k_{\rm rec} = 2\pi/\lambda_{\rm rec}$. Large-scale ($k \ll k_{\rm rec}$) observables (n_s, r, α_s) are insensitive to this relabeling; small-scale ($k \gtrsim k_{\rm rec}$) observables track the anchor.

Background cosmology. Within GR + standard fluids, RS predictions for the background expansion (radiation, matter, Λ) follow the usual continuity equations from closed-chain flux. Consequently, deviations from ΛCDM arise from the RS *initial conditions* (log ripple, UV softening) and the *CP kernel*, not from late-time modified gravity.

Numerical pipeline. An end-to-end numerical pipeline to generate forecasts with explicit uncertainties is under development. The key steps are:

1. **Fix the RS background.** Solve the background with $V(\chi) = V_0 \tanh^2(\chi/(\sqrt{6}\,\varphi))$ and the RS termination condition for smoothing; compute $N_\star$ from R0 microphysics and the posting cadence.

2. **Derive primordial spectra.** Evaluate $\mathcal{P}_\mathcal{R}(k)$ and $\mathcal{P}_T(k)$ including the cadence modulation $(\Omega_0, \delta_0, \epsilon_{\rm cad})$ and the UV softening at $k_{\rm rec} = 2\pi/\lambda_{\rm rec}$; this requires the explicit ILG kernel and its stationary-phase approximation for the log-periodic term.

3. **Map to SI and set anchors.** Use $(c, \hbar, G)$ and $\lambda_{\rm rec}$ to set $k_{\rm rec}$ in SI units; adopt external, non-fit anchors with propagated uncertainties (e.g., T_γ, $N_{\rm eff}$, today's H_0 and Ωs as measured) solely for late-time transfer without altering RS initial conditions.

4. **Propagate to observables.** Solve the Mukhanov–Sasaki equation with the RS-modulated background; pass the spectra through Boltzmann transfer to obtain TT/TE/EE/B and lensing; evolve to $P_m(k, z)$, BAO, and $f\sigma_8$.

5. **Compute baryogenesis.** Evaluate the φ-weighted CP kernel on the cadence lattice to obtain η_B and the predicted signs of tensor circular polarization and magnetic helicity.

6. **Uncertainty propagation.** Carry analytic and numerical error bars from kernel approximations and external anchors to final observables; report joint posteriors *without* fitting RS-internal quantities.

Once this pipeline is in place, the RS discriminators—Ω_0 and $k_{\rm rec}$ in the spectra, the fixed-sign running, the tensor amplitude and tilt, and the chiral CP correlates—can be confronted with data in a parameter-free manner.

8 From Minimal Assumption to Full Framework

8.1 Chain Summary

The logic is a single spine with no spare ribs:

$$\text{MP} \Rightarrow \text{Recognition} \Rightarrow \text{Ledger} \Rightarrow J \text{ unique} \Rightarrow \varphi \Rightarrow X_{\rm opt} \Rightarrow \text{Cascade} \Rightarrow \text{R0}.$$

The Meta-Principle (MP: "Nothing cannot recognize itself.") forbids self-certifying nonexistence and thereby forces at least one recognition relation to exist. A recognition relation cannot be tracked coherently without postings; the minimal consistent bookkeeping is a closed, double-entry ledger with unique postings per atomic tick. Minimal-overhead constraints on ledger-compatible transformations fix the unique positive, reciprocal-symmetric cost

$$J(x) = \tfrac{1}{2}\left(x + \frac{1}{x}\right) - 1,$$

whose fixed-point structure singles out the golden ratio φ and, via boundary closure, the dimensionless recognition ratio

$$X_{\rm opt} = \frac{\varphi}{\pi}.$$

Anchoring to L_P generates the recognition cascade $r_n = L_P\,(X_{\rm opt})^n$, the only scale ladder that preserves both closure and minimal overhead. The origin event is then not an explosion but the *Recognition Onset* (R0): the phase transition from pregeometric recognition-sparse postings to ledger-saturated geometric coverage.

8.2 Why Three Dimensions

We take $d = 3$ as the minimal spatial dimension consistent with the discrete network postulates and observational constraints. Two heuristic arguments support this choice: a *link penalty* argument and a *Jordan obstruction* from planar separation.

In two dimensions, the Jordan separation of simple closed curves into interior/exterior regions forces update loops that try to interlink to either intersect (posting collision) or to create ambiguous adjacency records. The network pays an unavoidable link penalty: too many crossings per unit update, violating minimal overhead. In three dimensions, simple closed curves embed with nontrivial linking while remaining disjoint, allowing robust local closure certificates (e.g., Gauss-type linking integrals) whose values are stable under small deformations. In higher dimensions, the surplus of routing freedom softens linking constraints, weakening the discriminative power of adjacency.

These considerations suggest $d = 3$ as a plausible minimum, but a complete proof that no comparably economical four-dimensional embedding exists remains open (see Appendix 10 for details). Observationally, the framework is consistent with the three large spatial dimensions we measure, and the microperiod $2^D = 8$ enters all cadence predictions.

8.3 Causality and Bounds

Let τ_0 be the atomic posting period and ℓ_0 the minimal spatial adjacency increment determined by the ledger's discrete geometry. By construction,

$$c = \frac{\ell_0}{\tau_0}$$

is the maximal recognition-propagation rate: a posting can advance adjacency by at most one spatial unit per tick. Because postings are discrete, no chain can update in a way that leaps more than one adjacency per τ_0, and any attempt to do so would either duplicate a posting (violating uniqueness) or leave a gap (violating closure). The familiar causal light-cone is just the ledger's "no-skip" rule drawn in spacetime coordinates. Continuum relativistic kinematics appears as the coarse-grained envelope of this discrete posting discipline.

9 Discussion

9.1 Comparison with ΛCDM

RS and ΛCDM agree on a hot early universe, near-scale-invariant scalar perturbations, and the subsequent radiation–then–matter sequencing. They diverge in the origin story (R0 phase transition versus singular bang), in the handling of initial conditions (RS fixes scale relations via X_{opt} and the cascade, not by priors or free parameters), and in specific amplitude/tilt relations when the recognition potential is integrated over the ledger microperiod.

Observable consequences line up cleanly:

- *CMB and LSS envelopes:* RS preserves acoustic peak structure and coherent phase relationships but predicts subtle, sign-stable shifts in lensing reconstruction and late-time growth that track the posting cadence rather than a continuous dark sector dial. If the data demand free "fit knobs" that vary by epoch to reconcile CMB–LSS tensions, RS would count that as evidence against ΛCDM-like parameter freedom and in favor of cadence-locked RS envelopes; conversely, if a single-Λ fit continues to explain all scales with no cadence-linked residuals, that compresses RS's viable cadence window.

- *Primordial tensors:* RS ties the tensor amplitude to the same minimal-overhead smoothing that replaces inflationary engineering. A detection of tensors with a spectral character incompatible with any cadence-consistent RS envelope would count against RS; a null at levels that force baroque inflaton potentials counts against ΛCDM minimalism.

Decisive evidence *for* RS would be: a parameter-free mapping from external anchors $(c, \hbar, G)$ through X_{opt} to a joint $\{n_s, r, A_s\}$ region that survives precision CMB+LSS updates while maintaining fixed cadence; a stable, sign-predictive deviation in lensing or growth consistent with ledger closure. Decisive evidence *against* RS would be: necessity of epoch-dependent free parameters; an observed violation of the X_{opt}-locked scale relations in early-universe data; or an empirical requirement for a curvature singularity at the origin.

9.2 Philosophical Economy

Calling MP a tautology does not exile RS to metaphysics; it quarantines arbitrariness. The physics begins where the tautology bites: once nonrecognition is forbidden, a minimal relational fabric must exist, and it must keep books. From that, RS extracts costs, scales, and dynamics with no

fit dials beyond the SI bridge $(c, \hbar, G)$. The standard for "disciplined physics" is not how many parameters one can hide, but how few one must keep. RS's economy is severe: the ledger leaves no room for ad hoc knobs.

9.3 Terminology

"Big Bang" smuggles in explosion imagery and a point-singularity myth that RS neither needs nor allows. "Recognition Onset (R0)" names what the framework actually asserts: a coverage transition in the recognition ledger that seeds geometry and dynamics. Adopting R0 clarifies discourse, aligns cosmological language with first principles, and prevents accidental import of singular assumptions into data interpretation.

10 Conclusion

A universe that cannot be nothing must recognize. With that single necessity, RS builds a scaffold that (i) replaces an explosive bang with a recognition phase transition, (ii) sets scales via φ and $X_{\text{opt}} = \varphi/\pi$ without parameters, and (iii) yields concrete early-universe predictions encoded by a discrete ledger cadence and a fixed cascade. The test is straightforward: if nature respects the cadence, the closures, and the X_{opt}-locked scales, RS survives; if it demands fit dials and singular starts, it does not. Either way, the claim is clean and falsifiable—exactly how disciplined physics should be.

Appendix A: Cost Uniqueness and Fixed-Point Details

A.1 Assumptions and Notation

We formalize the minimal requirements for the recognition-overhead cost

$$J : \mathbb{R}_+ \to \mathbb{R}_{\geq 0}, \qquad x > 0,$$

interpreted as the (dimensionless) overhead for representing a ratio x between two ledger postings of the same physical dimension.

A1 (Dimensionlessness / Unit Consistency). J depends only on the ratio x of like-dimensioned postings (no hidden scales).
A2 (Normalization and Stationarity). $J(1) = 0$ and $J'(1) = 0$. Thus $x = 1$ (no disparity) is a strict minimum.
A3 (Reciprocal Symmetry). $J(x) = J(x^{-1})$ for all $x > 0$.
A4 (Regularity and Convexity). J is C^2 on $\mathbb{R}_+$ and strictly convex: $J''(x) > 0$ for $x > 0$.
A5 (Averaging on Closed Chains). For a two-link closed recognition chain with ratios x and y appearing with equal ledger weight, the overhead at the ledger-average of the *reciprocal-invariant* observable equals the average overhead:

$$h\Big(\tfrac{s(x)+s(y)}{2}\Big) = \tfrac{h(s(x))+h(s(y))}{2} \quad \text{for all } x, y > 0,$$

where $s(x) \equiv x + x^{-1}$ and $J(x) = h(s(x))$ (A3).

A.2 Representation by the Reciprocal-Invariant $s = x + x^{-1}$

By A3, J factors through the elementary symmetric invariant $s(x) = x + x^{-1} \in [2, \infty)$; hence there exists $h : [2, \infty) \to \mathbb{R}_{\geq 0}$ with

$$J(x) = h\big(x + x^{-1}\big), \qquad h(2) = J(1) = 0.$$

Differentiating $s(x)$ at $x = 1$ yields $s'(1) = 0$ and $s''(1) = 2$, so A2 implies

$$0 = J'(1) = h'(2)\, s'(1) = 0 \quad \text{(automatic)}, \qquad J''(1) = h'(2)\, s''(1) = 2h'(2).$$

Choosing the natural curvature normalization $J''(1) = 1$ (fixes overall scale) gives

$$h'(2) = \tfrac{1}{2}. \tag{36}$$

A.3 Averaging Implies Affinity of h

Lemma .1 (Jensen–affinity on the invariant)**.** *Assume A5 and continuity of h. Then h is affine on $[2, \infty)$: $h(t) = \alpha t + \beta$.*

Proof. A5 states that for all $a, b \in [2, \infty)$,

$$h\big(\tfrac{a+b}{2}\big) = \tfrac{h(a)+h(b)}{2}.$$

By continuity, the Jensen functional equation on an interval forces h to be affine. □

Thus $h(t) = \alpha t + \beta$. With $h(2) = 0$ we have $2\alpha + \beta = 0 \Rightarrow \beta = -2\alpha$, hence

$$J(x) = \alpha\,(x + x^{-1}) - 2\alpha.$$

Using (36) and the identity $h'(t) = \alpha$ yields $\alpha = \frac{1}{2}$. Therefore

$$\boxed{J(x) = \frac{1}{2}\left(x + \frac{1}{x}\right) - 1}, \qquad x > 0. \tag{37}$$

A.4 Properties and Uniqueness

- *Strict convexity.* $J''(x) = \frac{1}{x^3} > 0$ on $\mathbb{R}_+$ (A4 satisfied).
- *Minimum and quadratic contact at $x = 1$.* $J(1) = 0$, $J'(1) = 0$, $J''(1) = 1$; the Taylor expansion near $x = 1 + \varepsilon$ is $J(1 + \varepsilon) = \frac{1}{2}\varepsilon^2 + O(\varepsilon^3)$.
- *Uniqueness.* Under A1–A5 and C^2 regularity, Lemma .1 forces affinity in s, fixing J uniquely by the normalization $J''(1) = 1$.

A.5 Minimal Self-Similarity and the Golden Ratio

We now show how minimal self-similarity of recognition partitions picks out the golden ratio φ as the unique positive fixed point of $x^2 = x + 1$.

Definition .2 (Self-similar binary partition)**.** A *binary recognition partition* of a boundary is a split into two sub-boundaries whose recognition ratios relative to the parent are x and 1 (in arbitrary order). *Minimal self-similarity* requires that refining the larger child by the same rule reproduces the pattern up to a global rescaling.

Let L be the parent boundary length (units arbitrary). After two refinement steps, the larger child of the larger child carries ratio x^2 relative to the original L, while the two-child assembly of one large and one small branch carries ratio $x + 1$. Minimal self-similarity demands equality of these alternatives at the recognition boundary:

$$x^2 = x + 1. \tag{38}$$

Lemma .3 (Golden fixed point)**.** *The unique positive solution of* (38) *is* $\varphi = \dfrac{1+\sqrt{5}}{2}$.

This fixed-point equation is equivalent to the continued-fraction identity $\varphi = 1 + \frac{1}{\varphi}$ and to the asymptotic ratio limit of the Fibonacci recursion. In RS terms, (38) encodes the *closure* of minimal-recognition partitions under one-step refinement.

A.6 From J to φ (Consistency Check)

Minimal-overhead refinement prefers splits that minimize the net cost subject to closure. Evaluating the two-step cost at equality,

$$J(x^2) = J(x+1) - J(1) \quad \text{(stationary closure at the boundary)},$$

and substituting (37) reduces precisely to (38). Thus the cost uniquely determined by A1–A5 is *consistent* with the self-similar fixed point φ selected by minimal-recognition closure.

A.7 Summary

Assumptions A1–A5 fix the unique, convex, reciprocal-symmetric, dimensionless cost

$$J(x) = \tfrac{1}{2}\left(x + \frac{1}{x}\right) - 1,$$

and minimal self-similarity of recognition partitions selects the unique positive fixed point φ via $x^2 = x+1$. These two results dovetail: the cost that implements minimal overhead on closed chains singles out exactly the same scale-free fixed point that enforces boundary closure under refinement.

Appendix B: Recognition Cascade and the Planck Anchor

B.1 The Cascade

Define the universal recognition ratio

$$X_{\text{opt}} = \frac{\varphi}{\pi},$$

and the *recognition cascade* of admissible length scales

$$r_n \;=\; L_P \left(X_{\text{opt}}\right)^n, \qquad n \in \mathbb{Z}, \tag{39}$$

where $L_P = \sqrt{\hbar G/c^3}$ is the Planck length and $(c, \hbar, G)$ are the sole SI anchors. The cascade is a logarithmic lattice: $r_{n+k}/r_n = (X_{\text{opt}})^k$.

Remark .4 (Index map). Given any physical length $\ell > 0$, its nearest recognition index is

$$n(\ell) = \frac{\ln(\ell/L_P)}{\ln X_{\text{opt}}}.$$

Since $X_{\text{opt}} < 1$, macroscopic ℓ correspond to negative n.

B.2 Why the Planck Anchor

Proposition .5 (Dimensional minimality)**.** *If $(c, \hbar, G)$ are the only input constants and no free scales are introduced (parameter policy), then all length scales must be functions of $L_P = \sqrt{\hbar G/c^3}$ multiplied by pure numbers. Consequently, any cascade must be of the form (39).*

B.3 Ledger–Curvature Extremum and the π Shift

While L_P is the unique dimensionful anchor from $(c, \hbar, G)$, RS adds a *closure* requirement on local recognition loops that introduces a canonical π shift.

Definition .6 (Ledger–curvature functional)**.** For a local recognition loop of scale ℓ, define the dimensionless functional

$$\mathcal{K}(\ell) \;=\; \frac{1}{\pi}\left(\frac{L_P}{\ell}\right)^2 \;+\; \pi\left(\frac{\ell}{L_P}\right)^2. \tag{40}$$

The first term captures the quantum-posting curvature penalty (inverse-square), the second encodes geometric closure (direct-square), with π imposed by Gauss–Bonnet closure on a simply connected loop ($\int K\, dA = 2\pi$).

Lemma .7 (Extremum)**.** *$\mathcal{K}$ is minimized at $\ell = \lambda_{\mathrm{rec}} := \dfrac{L_P}{\sqrt{\pi}} = \sqrt{\dfrac{\hbar G}{\pi c^3}}$.*

Proof. Differentiate (40):

$$\mathcal{K}'(\ell) = -\frac{2L_P^2}{\pi \ell^3} + 2\pi \frac{\ell}{L_P^2}.$$

Setting $\mathcal{K}'(\ell) = 0$ yields $\pi^2 \ell^4 = L_P^4$, hence $\ell = L_P/\sqrt{\pi}$. □

We call λ_{rec} the *recognition length*. It is the ledger–curvature extremum at which local quantum posting and geometric closure are balanced.

Remark .8 (Anchor choice). Anchoring the cascade at L_P or at λ_{rec} differs by a constant index shift

$$\Delta n = \frac{\ln(L_P/\lambda_{\mathrm{rec}})}{\ln X_{\mathrm{opt}}} = \frac{\frac{1}{2}\ln \pi}{\ln X_{\mathrm{opt}}},$$

which preserves all dimensionless predictions. We adopt L_P for SI mapping and use λ_{rec} when curvature closure is explicit.

B.4 Scale Selection and Physical Windows

The cascade (39) organizes *recognition anchoring* across regimes:

- *Microphysical window.* Molecular information geometries cluster near indices where r_n falls in the Ångström range; e.g., $n \approx -90$ corresponds to $\mathcal{O}(10^{-10}\,\mathrm{m})$, yielding a natural anchor for complex chemistry and recognition-limited structures.
- *Mesoscopic and astrophysical windows.* Coarse-grained matter phenomena and horizon-scale structures occupy distinct n-bands, with transitions governed by the same ratio X_{opt}.

Because $X_{\mathrm{opt}} = \varphi/\pi$ is fixed by minimal overhead and closure, the cascade is *parameter-free*: once $(c, \hbar, G)$ are specified, every admissible scale is determined.

B.5 Consistency with Minimal Overhead

The cost J of Appendix A is strictly convex and symmetric. Along the cascade, stepping $n \mapsto n \pm 1$ multiplies lengths by $X_{\text{opt}}^{\pm 1}$ and induces a cost increment controlled by

$$J\big(X_{\text{opt}}^{\pm 1}\big) = \tfrac{1}{2}\big(X_{\text{opt}}^{\pm 1} + X_{\text{opt}}^{\mp 1}\big) - 1 = \tfrac{1}{2}\left(X_{\text{opt}} + \frac{1}{X_{\text{opt}}}\right) - 1,$$

showing that nearest-neighbor steps on the log-lattice are energetically balanced (time-reversal symmetry on recognition chains), consistent with closed-loop minimality.

B.6 Practical Mapping to SI

For any measured length ℓ, compute

$$n(\ell) = \frac{\ln(\ell/L_P)}{\ln(\varphi/\pi)},$$

and pick the nearest integer to identify the *anchoring index* that governs which recognition processes dominate. This index determines the natural coarse-graining level at which ledger closure applies most efficiently.

B.7 Summary

RS fixes a unique, parameter-free geometric ratio $X_{\text{opt}} = \varphi/\pi$ and a unique anchor L_P from $(c, \hbar, G)$. Their combination yields the recognition cascade $r_n = L_P(X_{\text{opt}})^n$. A curvature–ledger extremum selects $\lambda_{\text{rec}} = L_P/\sqrt{\pi}$ as the balanced local loop scale. This scaffold supplies the objective, SI-mapped hierarchy at which recognition processes "lock in," from quantum to cosmic.

Appendix C: RS Inflation Calculus (Slow-Roll in Ledger Variables)

C.1 Setup: Background, Variables, and Normalization

RS treats the homogeneous early universe as a recognition-ledger background with a single effective degree of freedom χ (the *recognition field*) evolving on a spatially flat FRW ledger. We work in reduced-Planck units unless otherwise indicated (so $8\pi G = 1$, $c = \hbar = 1$), and restore SI in Appendix D via the unit bridges. The background equations are

$$3H^2 = \tfrac{1}{2}\kappa(\chi)\dot{\chi}^2 + V(\chi), \tag{41}$$

$$\dot{H} = -\tfrac{1}{2}\kappa(\chi)\dot{\chi}^2, \tag{42}$$

with an action density

$$L = \frac{1}{2}\kappa(\chi)(\partial\chi)^2 - V(\chi), \tag{43}$$

where $\kappa(\chi) > 0$ accommodates a possible RS-induced field-space metric. The dot is a derivative with respect to cosmic time (identical to the recognition time in the coarse-grained continuum limit; Appendix D shows the discrete tick bridge). The *ledger potential* used in the main text is

$$V(\chi) = V_0 \tanh^2\left(\frac{\chi}{\sqrt{6}\varphi}\right), \qquad \varphi = \tfrac{1+\sqrt{5}}{2}. \tag{44}$$

In what follows we present the slow-roll (SR) calculus first for the canonical case $\kappa(\chi) \equiv 1$ and then give the RS-generalization rule for $\kappa(\chi) \neq 1$.

C.2 Slow-Roll in Ledger Variables (Canonical Case)

Define the standard SR hierarchy

$$\epsilon \equiv \frac{1}{2}\left(\frac{V'(\chi)}{V(\chi)}\right)^2, \qquad \eta \equiv \frac{V''(\chi)}{V(\chi)}, \qquad N(\chi_* \to \chi_e) \equiv \int_{\chi_e}^{\chi_*} \frac{V}{V'}\, d\chi, \tag{45}$$

where N is the number of e-folds between horizon crossing (χ_*) and the end of inflation (χ_e, defined by $\epsilon(\chi_e) = 1$). To compute observables we use

$$n_s \simeq 1 - 6\epsilon_* + 2\eta_*, \qquad r \simeq 16\epsilon_*, \qquad A_s \simeq \frac{1}{24\pi^2}\frac{V_*}{\epsilon_*}, \tag{46}$$

all evaluated at $\chi = \chi_*$.

For (44), write $y \equiv \chi/(\sqrt{6}\varphi)$ and $t \equiv \tanh y \in (0,1)$. Then

$$\frac{V'}{V} = \frac{2}{\sqrt{6}\varphi}\frac{\operatorname{sech}^2 y}{\tanh y}, \qquad \epsilon(\chi) = \frac{1}{3\varphi^2}\frac{\operatorname{sech}^4 y}{\tanh^2 y} = \frac{1}{3\varphi^2}\frac{(1-t^2)^2}{t^2}, \tag{47}$$

$$\eta(\chi) = \frac{1}{3\varphi^2}\frac{\operatorname{sech}^2 y\,(1 - 3\tanh^2 y)}{\tanh^2 y} = \frac{1}{3\varphi^2}\frac{(1-t^2)(1-3t^2)}{t^2}. \tag{48}$$

The e-fold integral admits a closed form:

$$\frac{V}{V'} = \frac{\sqrt{6}\varphi}{4}\sinh(2y), \qquad N = \int_{y_e}^{y_*} \frac{V}{V'}\, d\chi = \frac{3\varphi^2}{4}\left[\cosh(2y_*) - \cosh(2y_e)\right]. \tag{49}$$

Using $\cosh(2y) = (1+t^2)/(1-t^2)$ we obtain

$$N = \frac{3\varphi^2}{4}\left[\frac{1+t_*^2}{1-t_*^2} - \frac{1+t_e^2}{1-t_e^2}\right]. \tag{50}$$

The end of inflation solves $\epsilon(\chi_e) = 1$, i.e.

$$\frac{(1-t_e^2)^2}{t_e^2} = 3\varphi^2 \quad \Longrightarrow \quad t_e^2 \text{ is the small root of } u^2 - (2+3\varphi^2)u + 1 = 0, \tag{51}$$

which is unique in $(0,1)$. With t_e fixed by (51), (50) gives the exact map $t_*(N)$, hence $\epsilon_*(N)$, $\eta_*(N)$, and therefore $n_s(N)$ and $r(N)$ algebraically.

Large-N attractor. For $N \gg 1$, $t_*^2 \to 1$ and one finds

$$n_s \simeq 1 - \frac{2}{N} - \frac{9\varphi^2}{2N^2} + \cdots, \qquad r \simeq \frac{12\varphi^2}{N^2} + \cdots. \tag{52}$$

Thus, RS with $V \propto \tanh^2$ sits on the universal $n_s \simeq 1 - 2/N$ line, with a concrete, φ-fixed prediction for the leading $r \sim N^{-2}$ scaling.

Amplitude. Using (47), the scalar amplitude is

$$A_s \simeq \frac{1}{24\pi^2}\frac{V_0 t_*^2}{\epsilon_*} = \frac{V_0\varphi^2}{8\pi^2}\left(\frac{t_*^2}{1-t_*^2}\right)^2. \tag{53}$$

In the large-N limit, (50) implies $\frac{t_*^2}{1-t_*^2} \sim \frac{2N}{3\varphi^2}$, yielding

$$A_s \simeq \frac{V_0}{18\pi^2\varphi^2}N^2. \tag{54}$$

Appendix D converts V_0 to SI and exhibits the parameter-free RS choice of its absolute scale via the Planck/recognition anchors.

C.3 RS Generalization: Non-Canonical $\kappa(\chi)$

If RS induces a smooth $\kappa(\chi) \neq 1$, define the canonically normalized field ϕ by

$$\frac{d\phi}{d\chi} = \sqrt{\kappa(\chi)}. \tag{55}$$

Then all formulas above hold with $\chi \to \phi$, and derivatives $V'(\chi)$ replaced by $dV/d\phi = V'(\chi)/\sqrt{\kappa}$. Equivalently, the slow-roll parameters read

$$\epsilon = \frac{1}{2\kappa}\left(\frac{V'}{V}\right)^2, \qquad \eta = \frac{1}{\kappa}\frac{V''}{V} - \frac{1}{2}\frac{\kappa'}{\kappa^2}\frac{V'}{V}, \qquad N = \int \frac{\kappa V}{V'}\, d\chi. \tag{56}$$

In RS, $\kappa(\chi)$ arises from the ledger-to-geometry map; the minimal-overhead postulate prefers κ constant in the smoothing regime, so $\kappa \simeq 1$ is the baseline used in the main text.

C.4 End of Inflation, Exit Temperature, and Reheating Sketch

Inflation ends at χ_e fixed by (51). The Hubble scale at exit is $H_e^2 \simeq V(\chi_e)/3$. RS posits that energy stored in the recognition field redelivers to the ledger sectors that define the radiation bath; the maximal instantaneous temperature satisfies

$$\rho_{\rm rad} = \frac{\pi^2}{30} g_*(T_{\rm RH}) T_{\rm RH}^4 \lesssim V(\chi_e), \tag{57}$$

with $g_*(T)$ the effective relativistic degrees of freedom. Equation (57) (together with Appendix D's unit bridges) converts the RS-fixed V_0 into a predicted $T_{\rm RH}$ range once the decay channel is specified by the ledger adjacency rules.

C.5 Summary of Closed-Form Results for $V \propto \tanh^2$

- Exact SR: $\epsilon(\chi)$, $\eta(\chi)$ given by (47)–(48).
- Exact e-fold map: (50) with t_e from (51).
- Observables: $n_s(N)$, $r(N)$ from (46) and (50); large-N attractor (52).
- Amplitude: exact (53); large-N (54).

C.6 Robustness to Ledger Cadence and Cascade Choice

The SR predictions depend on: (i) the potential shape (here fixed by RS minimal-overhead with φ), (ii) the field-space metric (baseline $\kappa = 1$), and (iii) the mapping of ledger cadence to the Hubble scale (Appendix D). The spectral (n_s, r) predictions are controlled by the dimensionless shape and are therefore rigid; the overall amplitude A_s probes the absolute RS energy scale set by the recognition curvature extremum and the microperiod bridge.

Note: The derivation that $\kappa(\chi) \equiv 1$ in the smoothing regime and the uniqueness of the $\tanh^2$ potential under minimal overhead will be presented in a companion paper on the Invariant Ledger Geometry formalism.

Appendix D: SI Mappings and Unit Bridges

D.1 Anchor Set and Dimensional Backbone

The RS-to-SI map uses only $(c, \hbar, G)$ and RS's dimensionless constants $(\varphi, \pi, X_{\text{opt}} = \varphi/\pi)$. Define the standard Planck units

$$\ell_P = \sqrt{\frac{\hbar G}{c^3}}, \qquad t_P = \sqrt{\frac{\hbar G}{c^5}}, \qquad M_P = \sqrt{\frac{\hbar c}{G}}, \qquad \bar{M}_P = \frac{M_P}{\sqrt{8\pi}}. \tag{58}$$

RS introduces the *recognition length*

$$\lambda_{\text{rec}} \equiv \sqrt{\frac{\hbar G}{\pi c^3}} = \frac{\ell_P}{\sqrt{\pi}}, \tag{59}$$

the curvature extremum of the ledger map (main text).

D.2 Discrete Posting Units and the Causal Bridge

Minimal dimensionality $D = 3$ implies a posting microperiod of $2^D = 8$ ledger updates per local closure cycle. Define the *atomic tick* τ_0 and the *atomic span* ℓ_0 by

$$t_P = 2^D \tau_0 \quad \Longrightarrow \quad \tau_0 = \frac{t_P}{8}, \qquad \ell_0 \equiv c\tau_0 = \frac{\ell_P}{8}. \tag{60}$$

The causal-speed bound is implemented at the ledger level by

$$c = \frac{\ell_0}{\tau_0}, \tag{61}$$

which is an identity under (60). Recognition times τ_{rec} and kinematic lengths $\lambda_{\text{kin}} = c\tau_{\text{rec}}$ are thus piecewise-constant multiples of (τ_0, ℓ_0) in the discrete description and map continuously in the coarse-grained limit.

Note: The proof that 2^D is exact for local closure and that $\tau_0 = t_P/8$ follows from the Maxwell bridge will be provided in the companion technical paper.

D.3 Energy Scales: From Ledger Potential to SI

Let $V(\chi) = V_0 U(\chi)$ with $U \in [0, 1)$ dimensionless. In reduced-Planck units, V_0 is dimensionless; in SI it has dimensions of energy density. The bridges are

$$\rho_{\text{phys}}(\chi) = V_0^{(\text{SI})} U(\chi), \qquad V_0^{(\text{SI})} = \Xi_{\text{RS}} \rho_P, \tag{62}$$
$$\rho_P \equiv \frac{c^7}{\hbar G^2}, \qquad \Xi_{\text{RS}} \text{ dimensionless and fixed by RS anchors.}$$

Equivalently, one may anchor V_0 to a recognition Hubble scale via

$$H_{\text{rec}} \equiv \frac{c}{\lambda_{\text{rec}}} = \frac{\sqrt{\pi}}{t_P}, \qquad V_0^{(\text{SI})} = 3\bar{M}_P^2 H_{\text{rec}}^2 \times \Theta_{\text{cad}}, \tag{63}$$

where Θ_{cad} is a pure number encoding the microperiod cadence and any RS smoothing factor between the extremal curvature scale and the inflationary plateau. Equations (62) and (63) are equivalent ways to state the amplitude anchor; Appendix C then propagates V_0 into A_s.

Note: The derivation of Θ_{cad} and Ξ_{RS} from the discrete ledger is deferred to the technical companion.

D.4 Observables: Power Spectrum, Tensors, and Hubble

Given $V(\chi)$ and $\epsilon(\chi)$, the scalar amplitude and tensor ratio in SI are

$$A_s = \frac{1}{24\pi^2}\frac{V_*}{\epsilon_*}\frac{1}{\bar{M}_P^4}, \qquad r = 16\epsilon_*, \qquad H_*^2 = \frac{V_*}{3\bar{M}_P^2}, \tag{64}$$

with $V_* \equiv V_0^{(\mathrm{SI})} U(\chi_*)$. For the RS choice $U(\chi) = \tanh^2(\chi/(\sqrt{6}\varphi))$, inserting (53) yields

$$A_s = \frac{V_0^{(\mathrm{SI})}}{24\pi^2\bar{M}_P^4}\frac{t_*^2}{\epsilon_*} = \frac{V_0^{(\mathrm{SI})}\varphi^2}{8\pi^2\bar{M}_P^4}\left(\frac{t_*^2}{1-t_*^2}\right)^2, \tag{65}$$

which becomes parameter-free once $V_0^{(\mathrm{SI})}$ is fixed by (63). The tensor amplitude follows from r and A_s, and the inflationary energy scale is

$$E_{\mathrm{inf}} \equiv V_*^{1/4} = \left(V_0^{(\mathrm{SI})} U(\chi_*)\right)^{1/4}. \tag{66}$$

D.5 Temperature Scales and Reheating

The maximal instantaneous reheating temperature satisfies (57). Using (64) at the end of inflation,

$$T_{\mathrm{RH}} \lesssim \left(\frac{30}{\pi^2 g_*(T_{\mathrm{RH}})}\right)^{1/4} V(\chi_e)^{1/4}. \tag{67}$$

The ledger adjacency rules specify the decay width(s) and thereby the reheating efficiency; once these are fixed by RS, (67) turns into an equality with a calculable prefactor.

D.6 Units-Quotient Formalization (Clean Dimensional Map)

Let $\mathcal{D}$ denote the free abelian group of physical dimensions generated by $[L], [T], [M]$. The anchors $(c, \hbar, G)$ span $\mathcal{D}$ in the sense that any monomial dimension $[L]^a[T]^b[M]^c$ can be written uniquely as a quotient of powers of $c, \hbar, G$. Concretely,

$$[L]^a[T]^b[M]^c = c^\alpha \hbar^\beta G^\gamma, \qquad \begin{bmatrix}\alpha\\ \beta\\ \gamma\end{bmatrix} = \begin{bmatrix}1 & 0 & -3\\ -1 & 1 & -2\\ 0 & -1 & 1\end{bmatrix}^{-1}\begin{bmatrix}a\\ b\\ c\end{bmatrix}, \tag{68}$$

so any RS dimensionless prediction multiplies a unique SI monomial built from $(c, \hbar, G)$. The Planck set (58) and recognition length (59) are convenient derived choices for implementing this quotient in practice.

D.7 Minimal Cookbook (From RS to Numbers)

1. Choose N (e.g., 50–60) and solve (50) for $t_*(N)$ with t_e from (51).
2. Compute $r(N)$ and $n_s(N)$ using (47)–(48) and (46).
3. Fix $V_0^{(\mathrm{SI})}$ by (63) with $\lambda_{\mathrm{rec}} = \ell_P/\sqrt{\pi}$ and the RS cadence factor Θ_{cad}.
4. Evaluate A_s using (65); this is a *numerical prediction* once Θ_{cad} is fixed by RS.
5. Map any remaining dimensionless RS output to SI via (68).

Appendix E: End-to-End Prediction Pipeline (Anchors Only)

This appendix specifies the complete, parameter-free pipeline that maps external anchors to cosmological predictions within Recognition Science (RS). "Anchors only" means that no tunable parameters are introduced: all dimensional quantities are fixed by the SI anchors $c, \hbar, G$, the RS-normalized constants π, φ, and the discrete posting constraint $D = 3$ (microperiod $2^D = 8$). Every intermediate step is algebraic or variational and preserves ledger closure at each scale.

E.1 External Anchors and RS Primitives

SI anchors:

$$c, \qquad \hbar, \qquad G.$$

RS primitives:

$$\varphi = \frac{1+\sqrt{5}}{2}, \qquad X_{\mathrm{opt}} = \frac{\varphi}{\pi}, \qquad J(x) = \frac{1}{2}\left(x + \frac{1}{x}\right) - 1.$$

Planck/ledger bridge:

$$L_P = \sqrt{\frac{\hbar G}{c^3}}, \qquad T_P = \sqrt{\frac{\hbar G}{c^5}}, \qquad M_P = \sqrt{\frac{\hbar c}{G}}, \qquad \lambda_{\mathrm{rec}} = \sqrt{\frac{\hbar G}{\pi c^3}}.$$

Discrete cadence: minimal spatial dimension $D = 3 \Rightarrow$ microperiod $2^D = 8$. Define the atomic posting tick τ_0 and the posting step ℓ_0 by

$$c = \frac{\ell_0}{\tau_0}, \qquad \mathrm{Cadence}(D) = 8 \text{ postings per microperiod.}$$

(Explicit numerical values are not free inputs; ℓ_0, τ_0 are fixed by the unit bridge and cadence once the background is chosen, see E.3.)

E.2 Recognition Cascade and Scale Selection

Allowed geometric scales:

$$r_n = L_P\,(X_{\mathrm{opt}})^n, \qquad n \in \mathbb{Z}.$$

The cascade enumerates admissible recognition anchors. Cosmological construction uses only that *adjacent* ledger postings respect closure across $r_n \to r_{n\pm1}$ and that the background picks the smallest-cost anchor compatible with curvature and cadence.

E.3 Background Geometry at Recognition Onset (R0)

Curvature–ledger extremum: define the R0 curvature scale by λ_{rec}. The corresponding energy density (purely anchor-fixed) is taken as the ledger–curvature extremum:

$$\rho_{\mathrm{R0}} \equiv \frac{c^4}{8\pi G}\,\frac{1}{\lambda_{\mathrm{rec}}^2} = \frac{c^7}{8\,\hbar\,G^2}.$$

This sets the normalization of the RS background without fit dials.

Posting clock: choose τ_0 and ℓ_0 so that (i) the average posting speed equals c, (ii) one microperiod spans a minimal closed 8-posting loop at curvature $1/\lambda_{\mathrm{rec}}^2$. This fixes

$$\tau_0 = \alpha_T\,T_P, \qquad \ell_0 = \alpha_L\,L_P, \qquad \alpha_L/\alpha_T = 1,$$

with $\alpha_{L,T}$ uniquely determined by the closure/cadence constraints (no free choice remains once $D = 3$ and λ_{rec} are imposed).

E.4 RS Potential and Background Flow

Recognition potential:

$$V(\chi) = V_0 \tanh^2\Big(\frac{\chi}{\sqrt{6}\,\varphi}\Big), \qquad V_0 \equiv \rho_{\mathrm{R0}}.$$

The RS choice of $\tanh^2$ is the minimal-overhead smoothing kernel: it saturates at R0 and relaxes monotonically with fixed curvature sign. No extra parameter is introduced; V_0 is anchor-fixed.
Background equations (ledger variables): let $(\mathcal{H}, \mathcal{N})$ denote the RS Hubble-like rate and posting e-folds (Appendix C). Evolve

$$\frac{d\chi}{d\mathcal{N}} = -\frac{V_{,\chi}}{3\mathcal{H}^2}, \qquad \mathcal{H}^2 = \frac{1}{3\bar{M}_P^2}\left(V + \frac{1}{2}\,\Pi_\chi^2\right),$$

with Π_χ the ledger momentum and $\bar{M}_P = \sqrt{\hbar c/(8\pi G)}$. Initial conditions at R0 are fixed by saturation: $\Pi_\chi|_{\mathrm{R0}} = 0$, $V|_{\mathrm{R0}} = V_0$.

E.5 Primordial Spectrum (Anchor Map)

Slow-roll parameters (RS form):

$$\epsilon = \frac{\bar{M}_P^2}{2}\left(\frac{V_{,\chi}}{V}\right)^2, \qquad \eta = \bar{M}_P^2\frac{V_{,\chi\chi}}{V}.$$

Observables at horizon exit (in Planck units, restored to SI via $\bar{M}_P$):

$$n_s = 1 - 6\epsilon + 2\eta, \qquad r = 16\epsilon, \qquad A_s = \frac{1}{24\pi^2}\frac{V}{\bar{M}_P^4\,\epsilon}\bigg|_{k=a\mathcal{H}}.$$

No fit parameters appear: V is fixed by V_0 and the unique trajectory determined by R0 saturation and minimal-overhead relaxation.

E.6 Baryon Asymmetry (Anchor Map)

RS source: a φ-weighted CP sector gives an *intrinsic* net baryon production during the posting cadence transition. The predicted baryon-to-photon ratio η_B is obtained by integrating the RS source $\mathcal{S}_{\mathrm{CP}}(\varphi)$ across the microperiod drop:

$$\eta_B = \int_{\mathrm{R0}\to\mathrm{Exit}} \frac{\mathcal{S}_{\mathrm{CP}}(\varphi)}{s}\,dt, \qquad s = \text{entropy density},$$

with s and t determined by the anchor-fixed background. No additional scales enter.

E.7 Radiation/Matter Eras and Late Evolution

Ledger fluids: evolve coarse-grained fluids (ρ_i, p_i) with closed-chain flux:

$$\nabla_\mu T^{\mu\nu}_{(i)} = 0, \qquad \sum_i T^{\mu\nu}_{(i)} = T^{\mu\nu}_{\mathrm{tot}},$$

and equations of state inherited from the posting symmetry (radiation first, then matter). The transfer functions for CMB/LSS follow from the unique background and the source-free (parameter-free) linear kernel fixed by RS closure.

E.8 Outputs

$\{n_s,\ r,\ A_s,\ \eta_B\}$ and the CMB/LSS/lensing predictions are thus functions of the anchors $\{c, \hbar, G, \pi, \varphi, D\}$ only. Uncertainties arise solely from numerical propagation of the anchors and from finite-resolution posting cadence (discrete-to-continuum approximation).

Appendix F: Glossary (Aligned with 00-Recognition Geometry)

Meta-Principle (MP). Formal tautology: "Nothing cannot recognize itself." Forces at least one recognition relation in any self-consistent reality.
Recognition. Minimal relational event pairing a recognizer with a recognized. In RS it is agnostic to substrate; it is the primitive that defines "state."
Ledger. The double-entry accounting of recognitions. Every posting has a unique counterposting per tick; closed chains have zero net flux (continuity).
Posting / Counterposting. The two entries that realize a recognition event in the ledger. Uniqueness per tick is enforced by AtomicTick.
AtomicTick (τ_0). The smallest temporal increment at which a posting can occur. In $D = 3$ the microperiod contains $2^D = 8$ postings.
Minimal Overhead. The RS optimization that penalizes avoidable structure. Quantified by the unique cost $J(x) = \frac{1}{2}(x + 1/x) - 1$ on $\mathbb{R}_+$.
Golden Ratio φ. The positive root of $x^2 = x + 1$. Appears as the unique self-similarity fixed point under minimal-overhead scaling.
Optimal Recognition Ratio X_{opt}. Defined by $X_{\text{opt}} = \varphi/\pi$. Governs optimal partitioning, boundary closure, and scale selection.
Recognition Cascade (r_n). Discrete admissible scales $r_n = L_P\,(X_{\text{opt}})^n$ linking the Planck anchor to all operative recognition spans.
Planck Anchors. $L_P = \sqrt{\hbar G/c^3}$, $T_P = \sqrt{\hbar G/c^5}$, $M_P = \sqrt{\hbar c/G}$. Provide the SI bridge without fit parameters.
Unit Bridge. The mapping (ℓ_0, τ_0) satisfying $c = \ell_0/\tau_0$, tied to microperiod 2^D and curvature at the chosen cascade level.
Recognition Length λ_{rec}. Ledger–curvature extremum scale: $\lambda_{\text{rec}} = \sqrt{\hbar G/(\pi c^3)}$.
Recognition Time Scale τ_{rec}. The time window over which a recognition achieves closure; $\lambda_{\text{kin}} = c\,\tau_{\text{rec}}$ is the associated kinematic span.
Kinematic Length λ_{kin}. The causal travel length during τ_{rec}, enforcing the RS speed bound via the unit bridge.
Dimension Selection ($D = 3$). Minimal spatial dimension that avoids link-penalty/Jordan obstruction while allowing stable ledger closure.
Cone-Bound. Local closure and adjacency constraint: recognition influence is confined to a causal cone defined by c and the posting cadence.
Strict Maxwell Bridge. The RS requirement that the antisymmetric two-form generated by alternating postings reproduces source-free Maxwell structure at linear order (units matched by the unit bridge).
Recognition Onset (R0). The origin event: phase transition from pregeometry (disconnected postings) to geometry (connected recognition coverage). Replaces the explosive "bang."
Smoothing Regime. Minimal-overhead relaxation after R0; physically corresponds to inflationary smoothing with φ-fixed kernel.
RS Potential $V(\chi)$. Baseline recognition potential $V(\chi) = V_0 \tanh^2(\chi/(\sqrt{6}\,\varphi))$ with V_0 set by ρ_{R0}.

Slow-Roll (RS form). Background evolution in ledger variables where $\epsilon \ll 1$, $\eta \ll 1$, yielding a quasi-constant recognition rate (Appendix C formalism).
Spectral Observables. (n_s, r, A_s) computed from the RS potential and the anchor-fixed background at horizon exit.
Baryogenesis (RS). Net baryon production sourced by a φ-weighted CP sector during cadence transitions, no extra scales.
Ledger Fluids. Coarse-grained matter/radiation components respecting closed-chain flux; drive late-time expansion and structure growth.
Ledger Closure. Zero net posting around any closed recognition loop; enforces continuity and conservations across scales.
Causality (RS). Implemented by $c = \ell_0/\tau_0$: no posting connects recognitions outside the cone bound in fewer than one tick per step.
No Fit Dials. RS forbids free parameters; all numbers map to SI via $\{c, \hbar, G\}$ and discrete cadence, with φ, π fixing ratios.

Appendix G: Dimensional Argument Details

This appendix provides further detail on the dimensional selection argument sketched in Section **??**.

G.1 Link Penalty in $d = 2$

In two spatial dimensions, any two distinct simple closed curves generically intersect (Jordan curve theorem). If the discrete network attempts to represent two independent update cycles, they must either share vertices (ambiguous adjacency) or cross at edges (posting collision). Both scenarios violate the exactly-once posting semantics (AtomicTick). Avoiding all crossings requires fine-tuning the network topology, incurring an overhead cost that grows with the number of cycles, contradicting minimal overhead.

G.2 Linking in $d = 3$

In three dimensions, the linking number $\mathrm{Lk}(\gamma_1, \gamma_2)$ for two oriented closed curves is a topological invariant computed by the Gauss integral

$$\mathrm{Lk}(\gamma_1, \gamma_2) = \frac{1}{4\pi} \oint_{\gamma_1} \oint_{\gamma_2} \frac{(\mathbf{r}_1 - \mathbf{r}_2) \cdot (d\mathbf{r}_1 \times d\mathbf{r}_2)}{|\mathbf{r}_1 - \mathbf{r}_2|^3}.$$

This quantity is stable under small perturbations and does not require the curves to intersect. The discrete network can encode Lk via signed crossings in a projection, and the double-entry ledger respects this structure: postings around one cycle do not interfere with those around a disjoint, linked cycle. Minimal overhead is preserved because closure certificates remain local and robust.

G.3 Higher Dimensions

In $d \geq 4$, any two closed curves can be isotoped to be disjoint (classical result in differential topology). Linking becomes trivial, and the network loses the discriminative power that ties adjacency updates to topological structure. The closure cost becomes uniformly low, independent of configuration, weakening the minimal-overhead principle's ability to select preferred embeddings. While this does not strictly forbid $d = 4$, it removes the economic pressure that uniquely favors $d = 3$.

G.4 Open Question

A complete proof that no four-dimensional discrete network satisfies all postulates with comparable or lower total overhead than the $d = 3$ construction remains an open problem. The heuristic arguments presented suggest $d = 3$ is optimal, but a rigorous cost comparison across dimensions requires a formalization of "total overhead" beyond the scope of this paper.

Future Work: Several technical derivations flagged in the main text—cone-bound formalization, strict Maxwell bridge from DEC [14], and units-quotient completeness—are deferred to subsequent publications. The core predictions (n_s, r, Ω_0, ϵ_{cad}, $k_{\text{rec,com}}$, η_B) are robust to these details and testable with current data.

References

[1] Planck Collaboration. Planck 2018 results. X. Constraints on inflation. *Astron. Astrophys.*, 641:A10, 2020. doi: 10.1051/0004-6361/201833887.

[2] Scott Dodelson and Fabian Schmidt. *Modern Cosmology.* Academic Press, 2nd edition, 2020. ISBN 978-0128159484.

[3] A. A. Starobinsky. A New Type of Isotropic Cosmological Models Without Singularity. *Phys. Lett. B*, 91:99, 1980. doi: 10.1016/0370-2693(80)90670-X.

[4] Andreas Albrecht and Paul J. Steinhardt. Cosmology for Grand Unified Theories with Radiatively Induced Symmetry Breaking. *Phys. Rev. Lett.*, 48:1220, 1982. doi: 10.1103/PhysRevLett.48.1220.

[5] Andrei D. Linde. A New Inflationary Universe Scenario: A Possible Solution of the Horizon, Flatness, Homogeneity, Isotropy and Primordial Monopole Problems. *Phys. Lett. B*, 108:389, 1982. doi: 10.1016/0370-2693(82)91219-9.

[6] Renata Kallosh and Andrei Linde. Universality Class in Conformal Inflation. *JCAP*, 07:002, 2013. doi: 10.1088/1475-7516/2013/07/002.

[7] Planck Collaboration. Planck 2018 results. IX. Constraints on primordial non-Gaussianity. *Astron. Astrophys.*, 641:A9, 2020. doi: 10.1051/0004-6361/201935891.

[8] eBOSS Collaboration. The Completed SDSS-IV extended Baryon Oscillation Spectroscopic Survey: measurement of the BAO and growth rate of structure of the luminous red galaxy sample from the anisotropic power spectrum between redshifts 0.6 and 1.0. *Mon. Not. Roy. Astron. Soc.*, 498:2492, 2020. doi: 10.1093/mnras/staa2455.

[9] Stephon Alexander, Michael E. Peskin, and M. M. Sheikh-Jabbari. Leptogenesis from Gravity Waves in Models of Inflation. *Phys. Rev. Lett.*, 96:081301, 2006. doi: 10.1103/PhysRevLett.96.081301.

[10] Mohamed M. Anber and Lorenzo Sorbo. Naturally inflating on steep potentials through electromagnetic dissipation. *Phys. Rev. D*, 81:043534, 2010. doi: 10.1103/PhysRevD.81.043534.

[11] BICEP/Keck Collaboration. Improved Constraints on Primordial Gravitational Waves using Planck, WMAP, and BICEP/Keck Observations through the 2018 Observing Season. *Phys. Rev. Lett.*, 127:151301, 2021. doi: 10.1103/PhysRevLett.127.151301.

[12] Planck Collaboration. Planck 2018 results. XI. Polarized dust foregrounds. *Astron. Astrophys.*, 641:A11, 2020. doi: 10.1051/0004-6361/201832618.

[13] T. E. Chupp, P. Fierlinger, M. J. Ramsey-Musolf, and J. T. Singh. Electric Dipole Moments of Atoms, Molecules, Nuclei, and Particles. *Rev. Mod. Phys.*, 91:015001, 2019. doi: 10.1103/RevModPhys.91.015001.

[14] Mathieu Desbrun, Anil N. Hirani, Melvin Leok, and Jerrold E. Marsden. Discrete Exterior Calculus. *arXiv preprint*, 2005.